IL NUOVO CIMENTO **49 C** (2026) 146
DOI 10.1393/ncc/i2026-26146-8

COMMUNICATIONS: SIF Congress 2025

Tackling the problem of diffusion in Fricke gel dosimeters through a Physics-informed neural network algorithm

M. ROMEO(1)(2)(3) on behalf of G. COTTONE(1)(3), S. LOCARNO(4)(5), D. PASSERI(4)(5), I. VERONESE(4)(5), A. DE FARIAS SOARES(1)(3), M. C. D'OCA(1)(3)(6), G. MILLUZZO(3), F. ROMANO(3), C. GAGLIARDO(7)(8), F. DI MARTINO(9)(10)(11), F. D'ERRICO(11)(12)(13), C. LENARDI(4)(5) and M. MARRALE(1)(3)(6)

(1) *Dipartimento di Fisica e Chimica "Emilio Segré", Università di Palermo - Palermo, Italy*
(2) *Dipartimento di Scienze Biologiche, Chimiche e Farmaceutiche, Università di Palermo Palermo, Italy*
(3) *INFN, Sezione di Catania - Catania, Italy*
(4) *Dipartimento di Fisica Aldo Pontremoli, Università di Milano - Milan, Italy*
(5) *INFN, Sezione di Milano - Milan, Italy*
(6) *Advanced Technologies Network (ATen) Center - Palermo, Italy*
(7) *Dipartimento di Biomedicina, Neuroscienze e Diagnostica Avanzata, Univerità di Palermo Palermo, Italy*
(8) *Ospedale Policlinico "Paolo Giaccone" - Palermo, Italy*
(9) *Centro Pisano Ricerca e Implementazione Clinica Flash Radiotherapy, Presidio S. Chiara Pisa, Italy*
(10) *Fisica Sanitaria, Azienda Ospedaliero Universitaria Pisa AOUP - Pisa, Italy*
(11) *INFN, Sezione di Pisa - Pisa, Italy*
(12) *Dipartimento di Ingengeria Civile a Industriale, Università di Pisa - Pisa, Italy*
(13) *Magnetic Resonance Research Center, School of Medicine of Yale - New Haven, CT, USA*

received 7 February 2026

Summary. — The use of radiation in medical applications demands accurate dose measurements, particularly with the advent of high-dose rates and mini-beam fields. In this context, Fricke Gels (FGs) are gaining interest for their tissue-equivalent properties. FGs rely on Fe^{2+} to Fe^{3+} oxidation upon radiation exposure, that can be quantified by MRI or Optical Absorption (OA) spectroscopy, enabling access to 3D Dose Distributions (DD). Ion diffusion bring to blurring effects in the recorded DD. Furthermore adding chelating agents, such as methylthymol blue (MTB), induces auto-oxidation processes. Both physical phenomena strongly limit FG's clinical utility. Although the processes can be described by modified Diffusion Equation, reconstructing the backward time DD leads to a challenging inverse problem. A promising solution is given by the Physics-Informed Neural Networks (PINNs), which integrate physical laws with machine learning to solve partial differential equations. In this study, we trained PINNs to predict pre-diffusion DD in 1D MTB FGs, exploiting diffused data up to 8 hours post-irradiation. Predictions were compared with OA data from irradiated MTB-GTA gel. Results in terms of Mean Squared Error (MSE) (1×10^{-6}–$1\times10^{-5} OD^2$) indicate the PINNs potential in overcoming FG limitations.

TABLE I. – *Gel slices Summary.*

Sample ID	PVA mixture		
	% 18–88 $MW \sim 130$ kDa $HD \sim 88\%$	% 4–88 $MW \sim 31$ kDa $HD \sim 88\%$	% 20–98 $MW \sim 125$ kDa $HD \sim 98\%$
Gel A	100	–	–
Gel B	100	–	–
Gel C	30	70	–
Gel D	30	70	–
Gel E	30	–	70

1. – Description

Fricke Gels (FG) are well-known chemical dosimeters, which exploit Fe^{2+} oxidation into Fe^{3+} ions as proportional marker for ionizing radiation dose estimation [1]. By adding a chelating agent, such as methylthymol blue (MTB), the absorbed dose results being proportional to the variation of gel Absorbance at specific wavelength (600 nm). However, these dosimeters are affected by two physical-chemical phenomena: ion diffusion and Auto-Oxidation (AO) [2]. Both processes strongly limit the FG use in clinical applications: diffusion causes a blurring effect in measured Dose Distributions (DD), and AO breaks the linear relation ion concentration-absorbed dose. In both cases, the extent of the effects depends on the time interval between gel preparation/irradiation and measurements. This time interval can be very long due to measurements equipment logistics and availability.

Since the ion concentration behavior can be described by Partial Derivative Equations, in this work we propose the use of Physics-Informed Neural Networks (PINNs) [3] in order to solve the time diffusion problem [4, 5]. This approach can reconstruct the initial DD starting from the distribution at the generic time t_m (after irradiation) and given the diffusion coefficient.

The method is tested on different types of gels; the distances (Mean Squared Error) between the predicted and the experimentally measured profiles are in the range $1 \times 10^{-6} - 1 \times 10^{-5}$.

2. – Materials and methods

2˙1. *Gels preparation.* – FGs were prepared at the Department of Physics, University of Milan. Three types of hydrogels were produced by varying the equivalent molecular weight. After preparation, the gels were injected into planar PVC containers (referred to as "slices") of size $60 \times 60\,\mathrm{mm}^2$. Gels preparation followed the procedure and materials reported in [6], replacing Xylenol Orange tetrasodium salt with $0.2mM$ of MTB. Sample compositions are summarized in table I.

To limit AO, gels have been stored in a refrigerated environment at 4 °C during the experimental activities. Unfortunately, this precaution affected some measurements due to the presence of condensation on the glass of the slices.

2˙2. *Irradiation.* – The hydrogels were irradiated about 24 hours after preparation by a Varian Clinic-Unique linear accelerator (LINAC, Varian Medical System, CA, USA) at "Fondazione IRCCS Istituto Nazionale dei Tumori" in Milan. The gels were placed between a tissue-equivalent slice approximately 5 cm thick, at source to surface distance of about 50 cm. The delivered dose was about 8 Gy.

2˙3. *OD measurement.* – In Fricke dosimeters, the physical quantity related to the Absorbed Dose is the concentration of Fe^{3+} ions. When a chelating agent is incorporated into the gel, the Fe^{3+} ion concentration induces a color change, which can be measured as a variation in Absorbance (A) at specific wavelength. In the case of MTB, the wavelength was 600 nm. Gel reading was performed using a digital Gafchromic film scanner (Epson Perfection V850 Pro), which measures optical transmittance. Each acquisition produced an RGB image; only the red channel was retained for subsequent analysis. There is a direct linear relationship between the Absorbed Dose and the change in A [7,8], the latter expressed as

$$\Delta A = A_R - A_{NR} = log\left(\frac{I_{NR}}{I_R}\right) \tag{1}$$

where I stands for *gray-level* Intensity, and the subscripts R and NR refer to the irradiated (*i.e.*, exposed to ionizing radiation) and non-irradiated gel, respectively.

2˙4. *Data pre-processing.* –

2˙4.1. Image registration. Images were processed using the ImageJ software [9]. In particular, the gel image series were stacked using the "Stack" function and subsequently co-registered using a 2D rigid registration algorithm.

2˙4.2. Image cropping. After registration, to remove unusable details such as air bubbles and to mitigate irradiation border effects, the image series were cropped by removing 1 cm from each edge.

2˙5. *PINN method correction.* – PINNs are models trained to satisfy certain physical laws. Their functionality is based on the Universal Approximation Theorem concerning multilayer perceptron (MLP) neural network [10]. FG dose distribution are described by Diffusion equation. Let us denote the position vector as $\boldsymbol{x}$ in the spatial domain Ω representing the gel system, and the generic time $t \in [0, t_m]$, where t_m is the time interval between irradiation and measurement. Let $NN(\boldsymbol{x}, t; \boldsymbol{\theta})$ be a neural network with parameters $\boldsymbol{\theta}$. Randomly selecting N_1 points $(\boldsymbol{x_i}, t_i) \in \Omega \times [0, t_m[$ we can then define a residual loss function $\mathcal{L}_{res}$ as follows:

$$\mathcal{L}_{res} = \frac{1}{N_1} \sum_i \left(\frac{\partial}{\partial t} NN(\boldsymbol{x_i}, t_i; \boldsymbol{\theta}) - D\nabla^2 NN(\boldsymbol{x_i}, t_i; \boldsymbol{\theta}) \right)^2. \tag{2}$$

In the same way, the boundary condition loss function $\mathcal{L}_{BC}$ can be constructed randomly selecting N_2 points from $\partial\Omega \times [0, t_m[$, where $\partial\Omega$ is the boundary of Ω. Since Fe^{3+} ions cannot escape from the gel, we can impose Neumann boundary condition. It follows that:

$$\mathcal{L}_{BC} = \frac{1}{N_2} \sum_i (\hat{\boldsymbol{n}} \cdot \nabla NN(\boldsymbol{x_i}, t_i; \boldsymbol{\theta}))^2 \tag{3}$$

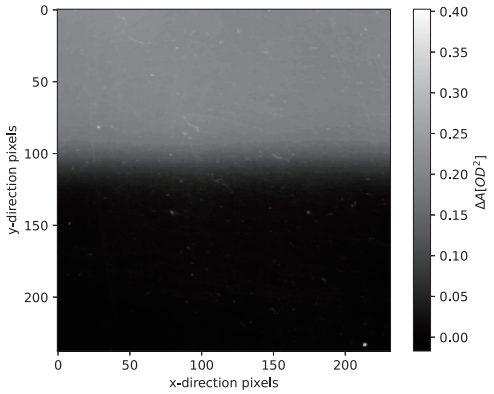

Fig. 1. – ΔA image for gel C at 0.8 h after irradiation. The image is obtained by applying eq. (1) pixel by pixel.

where $\hat{\boldsymbol{n}}$ is the unit vector normal to $\partial\Omega$.

Finally, the data-driven loss function $\mathcal{L}_{DD}$ is obtained by comparing the NN output with the experimental profile $P(\boldsymbol{x})$ at t_m,

$$\mathcal{L}_{DD} = \frac{1}{N_3}\sum_i \left(NN(\boldsymbol{x_i}, t_m; \boldsymbol{\theta}) - P(\boldsymbol{x_i})\right)^2, \tag{4}$$

where N_3 is the number of random points selected within the spatial domain.

Once the loss function $\mathcal{L} = \mathcal{L}_{res} + \mathcal{L}_{BC} + \mathcal{L}_{DD}$ is defined, finding the parameters $\boldsymbol{\theta}$ that minimize $\mathcal{L}$ corresponds to making the $NN(\boldsymbol{x}, t; \boldsymbol{\theta})$ an approximate solution to the backward-time diffusion problem associated with ion motion in FG [3, 11-13]. However, note that in this Boundary Value Problem the uniqueness solution is not guaranteed, this issue has been addressed in the references [4, 5].

2˙6. *Models training.* – PINN correction was applied to Gels A, B, C, D, and E using the following setup: a MLP with 5 hidden layers (shape = [10, 20, 200, 20, 10] and tanh as the activation function), the Adam optimizer, 30000 training epochs, and N1 = 20000, N2 = 20000, and N3 = 10000 random points per epoch sampled from the interior, the boundary, and the measurement at the time tm, respectively. The training duration for each gel is approximately half an hour on a workstation equipped with an NVIDIA GeForce RTX 4090 graphics processing unit. In order to maintain consistency, all profiles and estimated parameters were converted to standard physical units ([length] = mm and [time] = h) before being input into the neural network.

3. – Results

3˙0.1. Linear profile extrapolation. After image pre-processing, a representation of the variation of Absorbance can be obtained by applying eq. (1) between the reference image (acquired before irradiation) and the images acquired after irradiation. A representative example is depicted in fig. 1.

Images can be seen as matrices $M \times N$, where M is the number of pixel along the vertical direction (y) and N is the same number along the horizontal direction (x). This means that by selecting a column (x fixed) we can observe how Absorbance varies along

TABLE II. – *Diffusion coefficients estimation for gels used in linear DD.*

Gel slice	D [mm^2/h]	ΔD [mm^2/h]
Gel A	0.19	0.01
Gel B	0.21	0.01
Gel C	0.18	0.01
Gel D	0.20	0.01
Gel E	0.22	0.01

the y direction, providing a linear profile. Since the irradiation was uniform, the system exhibits translational invariance along the horizontal direction. Therefore, the best A estimate can be obtained by averaging the linear profiles along the x-direction.

This analysis was conducted for gels A,B,C,D, and E. As an illustrative example, the results of the signal as a function of pixel position along the y-direction in the image is shown below in fig. 2, for gel B at different times after irradiation (left panel).

As better evidenced in the insets in the left panel, the profile exhibits an upward shift over time. This behavior can be attributed to auto-oxidation effects. By evaluating the difference between the maximum and minimum measured Absorbance at each time point, the maximum relative deviation was found to be approximately 1% for each gel. This result enables to assume auto-oxidation to be uniform across the entire sample and justifies subtracting a baseline from each curve. The resulting linear profiles (fig. 2, right panel) now exhibit time-dependent changes driven solely by diffusion processes. Estimations for diffusion coefficients can be then performed in accordance to the methods proposed in [1, 14]. Results are reported in table II.

3˙1. *PINN method application.* – The PINN algorithm was applied to the latest measured linear profile (8.2 h after irradiation) to approximate the first measured (0.8 h after irradiation). This procedure was performed for gels A, B, C, D, and E. The result for gel B is shown in fig. 3. To provide a quantitative measure of the method's performance, we evaluate the distance (Mean Squared Error) between the prediction and the first mea-

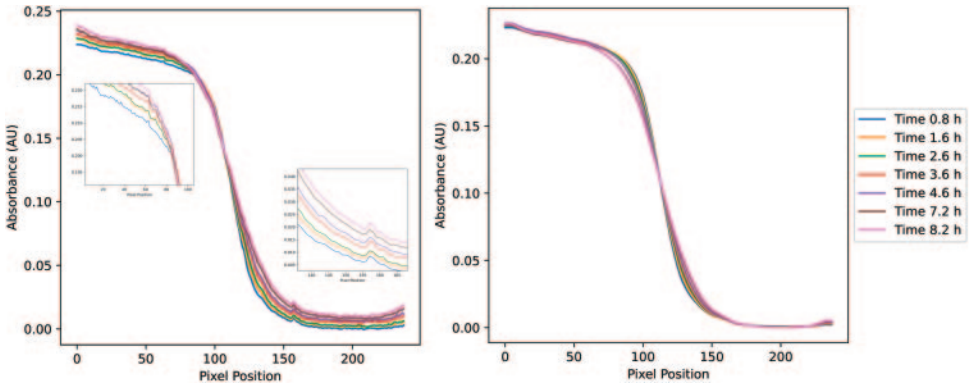

Fig. 2. – Left panel: raw absorbance linear profiles for Gel B. The insets show a zoom of the initial and final portions of the curves, highlighting the absorbance increase with time. Right panel: absorbance linear profiles after baseline subtraction and data smoothing.

surement, and compare it with the distance between the latest measurement and the first one. Results for all gels are shown in table III, and they indicate that the PINN model correction can reduce the MSE by an order of magnitude in many cases, demonstrating a clear advantage in using it.

4. – Discussion

In this work, we applied the approach proposed in references [4,5] to MTB-doped gels, which are also affected by AO. Based on the *a posteriori* observation of linear profiles, AO was removed by baseline subtraction. This allowed the problem to be reduced to a purely diffusive phenomenon. However, this approximation is limited to the present case. In particular, since irradiation induces an ion concentration gradient for both Fe^{2+} and Fe^{3+}, the assumption of spatially uniform AO holds only when the product of the AO rate and the experimental time scale is much smaller than the Fe^{2+} reserve. This condition depends on both the gel AO rate and the absorbed dose.

Furthermore, FGs are well known to be 3D dosimeters; however, in this study, symmetry considerations allowed us to reduce the problem to a 1D representation. In a previous work [5], the extension of the PINN method to higher dimensions was proposed for simulated 2D and 3D dose distributions. In the case of experimental dose distributions, many complications contribute to making the problem challenging. In particular, noise and local artifacts require specific imaging techniques and corrections, such as median filtering, to be properly addressed. Moreover, in the 2D and 3D cases, estimating the AO contribution would require in-depth theoretical modeling to be included into the PINN framework.

5. – Conclusion

Diffusion of Fe^{3+} ions combined with AO processes strongly limit FGs application in clinical fields, shortening their utilization time. Furthermore, logistics in clinics do not always allow for fast measurements. In this work we propose the PINN method as a solution to overcome this issue. Starting from the DD experimentally measured

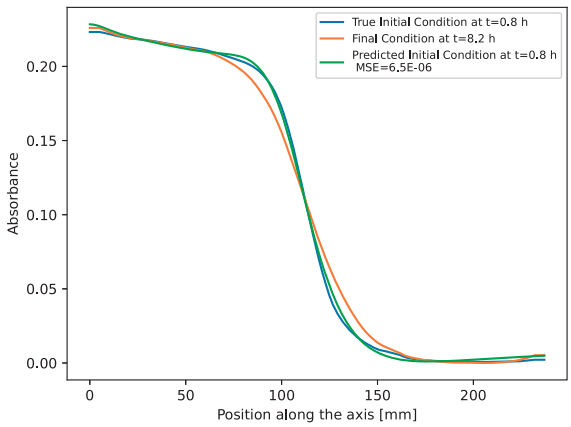

Fig. 3. – Results of the PINN model correction for gel B. It can be observed that the first profile (retrieved applying PINN algorithm from the latest) is almost fully recovered.

TABLE III. – *Comparison between the MSE of the first vs. latest profile and the MSE of the first profile vs. PINN correction.*

Sample ID	time first profile [h]	time last profile [h]	MSE last profile [OD^2]	MSE PINN correction [OD^2]
Gel A	0.8	8.2	5.1×10^{-5}	7.4×10^{-6}
Gel B	0.8	8.2	5.0×10^{-5}	6.5×10^{-6}
Gel C	0.8	8.2	4.2×10^{-5}	8.6×10^{-6}
Gel D	0.8	8.2	3.2×10^{-5}	8.8×10^{-6}
Gel E	0.8	8.2	5.7×10^{-5}	2.5×10^{-5}

post irradiation, our algorithm is able to approximate the distribution back in time. The consistent results obtained across different gel types highlight the robustness of the method.

* * *

This work was received funding from the Italian National Institute of Nuclear Physics with the research project Artificial Intelligence in Medicine (AIM_MIA). MR acknowledges funding from UPMC Italy srl.

REFERENCES

[1] MARRALE M. and D'ERRICO F., *Gels*, **7** (2021) 74.
[2] PENEV K. and MEQUANINT K., *J. Phys.: Confer. Ser.*, **444** (2013) 012105.
[3] LEE H. and KANG I. S., *J. Comput. Phys.*, **91** (1990) 110.
[4] ROMEO M. *et al.*, *Radiat. Meas.*, **175** (2024) 107171.
[5] ROMEO M., COTTONE G. *et al.*, *Gels*, **10** (2024) 565.
[6] LOCARNO S. *et al.*, *Gels*, **10** (2024) 172.
[7] PENEV K. and MEQUANINT K., *J. Phys.: Conf. Ser.*, **573** (2015) 012030.
[8] PENEV K. I. and MEQUANINT K., *Med. Phys.*, **44** (2017) 1948.
[9] COLLINS T. J., *BioTechniques*, **43** (2007) S25.
[10] HORNIK K., STINCHCOMBE M. and WHITE H., *Neural Netw.*, **2** (1989) 359.
[11] LAGARIS I. E., LIKAS A. and FOTIADIS D. I., *IEEE Trans. Neural Netw.*, **9** (1998) 987.
[12] RAISSI M., PERDIKARIS P. and KARNIADAKIS G. E., *J. Comput. Phys.*, **378** (2019) 686.
[13] KARNIADAKIS G. E. *et al.*, *Nat. Rev. Phys.*, **3** (2021) 422.
[14] KRON T., JONAS D. and POPE J. M., *Magn. Reson. Imaging*, **15** (1997) 211.